Clinical Investigative Study

Virtual Histology Analysis of Carotid Atherosclerotic Plaque: Plaque Composition at the Minimum Lumen Site and of the Entire Carotid Plaque

Arihito Tsurumi, MD, PhD, Yuko Tsurumi, MD, Osamu Hososhima, MD, Noriaki Matsubara, MD, PhD, Takashi Izumi, MD, PhD, Shigeru Miyachi, MD, PhD

From the Department of Neurosurgery, National Hospital Organization Nagoya Medical Center, Nagoya, Japan (AT); Department of Neurosurgery, Japanese Red Cross Nagoya Daiichi Hospital, Nagoya, Japan (YT); Department of Neurosurgery, Tosei General Hospital, Seto, Japan (OH); Department of Neurosurgery, Nagoya University Graduate School of Medicine, Nagoya, Japan (NM, TI, SM).

A B S T R A C T

BACKGROUND
Virtual Histology intravascular ultrasound (VH IVUS) volumetric analysis (analysis of the entire plaque responsible for stenosis) has been used for carotid plaque diagnosis. Knowing the carotid plaque characteristics by analyzing the plaque composition only at the minimum lumen site will facilitate plaque diagnosis using VH IVUS.

PURPOSE
To detect the relationship between the VH IVUS volumetric analysis of the entire plaque responsible for carotid artery stenosis and the VH IVUS cross-section plaque analysis at the minimum lumen site.

METHODS
Forty-eight atherosclerotic cervical carotid stenoses in 45 consecutive patients were included in the study. VH IVUS was obtained during the carotid artery stenting procedure.

RESULTS
Simple regression analysis revealed that the volumetric proportion of each plaque type correlated significantly with the corresponding plaque-type area at the minimum lumen site. The adjusted coefficients of determination of the simple regression analyses were .782 ($P < .001$) for fibrous tissue, .741 ($P < .001$) for fibrofatty tissue, .864 ($P < .001$) for dense calcium, and .918 ($P < .001$) for necrotic core.

CONCLUSION
The plaque composition at the minimum lumen site represents the volumetric composition of the entire carotid plaque that causes atherosclerotic cervical carotid artery stenosis.

Introduction

Echolucent carotid plaque is associated with procedural embolization during carotid artery stenting and neurological complications, and this dangerous plaque is called vulnerable plaque.[1-3] For the treatment of patients with carotid artery stenosis, plaque imaging to analyze plaque characteristics is important to detect vulnerable plaque and avoid ischemic complications. Magnetic resonance imaging,[4-7] computed tomography,[8,9] positron emission tomography,[10,11] carotid ultrasonography,[5] and intravascular ultrasound (IVUS)[12,13] have been reported as carotid plaque imaging devices. Conventional IVUS has been used for over a decade in carotid stenting, not only to assess the plaque before treatment, but also to measure arterial diameters and subsequently to assess the completeness of stent deployment. Virtual Histology (VH; Volcano Corporation, Rancho Cordova, CA), which is based on spectral and amplitude analyses of the IVUS radiofrequency backscatter signals, is an advanced radiofrequency analysis of IVUS signals.[3] Several studies of coronary[14-16] and carotid[3] artery plaque imaging have demonstrated that VH allows reliable identification of four atherosclerotic plaque types: fibrous, fibrofatty, dense calcium, and necrotic core. In addition, the geometric and compositional output of VH IVUS has been reported to be reproducible.[17] The VH cross-sectional images are created from both the intensity and frequency of the reflected ultrasound, with the frequencies varying according to the tissue types.[14] VH IVUS provides color-coded maps of four different histological components of plaque (green, fibrous; yellow, fibrofatty; white, dense calcium; and red, necrotic core) with the lumen colored black.[3,18]

VH IVUS has been used to evaluate plaque characteristics in both coronary interventions[19,20] and neurointerventions.[21-25]
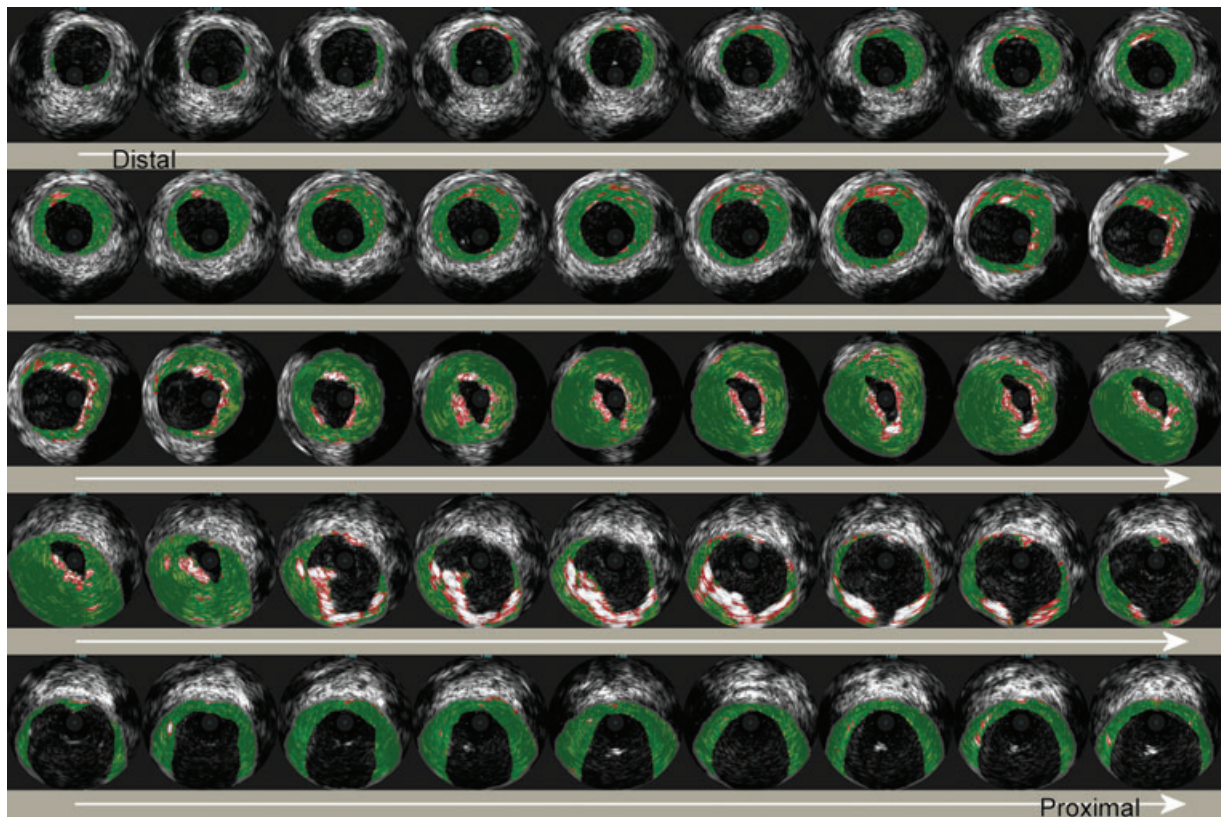
Fig 1. A VH IVUS sample image of color-coded plaque compositional maps on transverse planes in a patient with symptomatic internal carotid artery origin stenosis. VH IVUS shows a large fibrofatty necrotic core plaque with calcification. VH IVUS provides color-coded maps of four different histological components of plaque (green, fibrous; yellow, fibrofatty; white, dense calcium; and red, necrotic core), with the lumen colored black.

Rupture of vulnerable plaque in the coronary arteries is the cause of most acute coronary syndromes. VH IVUS can identify the vulnerable plaque by its high content of necrotic lipid core.[26] In addition, the authors have previously reported that periprocedural hypotension in carotid artery stenting can be predicted by VH IVUS volumetric analysis of the plaque responsible for the carotid artery stenosis. Fibrous plaque, in which fibrous tissue detected on VH IVUS is composed of more than 60% of the whole plaque volume on VH IVUS, is the independent risk factor for periprocedural hypotension (systolic blood pressure ≤ 90 mm Hg) and prolonged periprocedural hypotension (requiring vasopressor for >3 hours) in carotid artery stenting.[27]

VH IVUS volumetric analysis of the plaque, which can be achieved by performing integral analysis of the cross-sectional plaque analyses, is a time-consuming task. In contrast, analyzing only one cross-section at the minimum lumen site is easier and faster than VH IVUS volumetric analysis. If it is possible to know the carotid plaque characteristics by analyzing the plaque composition only at the minimum lumen site, plaque diagnosis using VH IVUS will become easier, and easier prediction of patients who will have periprocedural hypotension during carotid artery stenting will become possible. This study was conducted to identify the relationship between the volumetric analysis of the entire carotid plaque and one cross-section plaque analysis at the minimum lumen site.

Methods

Study Design

A retrospective, cross-sectional study of patients who underwent interventional therapy for cervical carotid artery stenosis in a tertiary referral hospital from April 1, 2006 to April 30, 2007 was conducted. All consecutive patients who underwent interventional therapy for cervical carotid artery stenosis in our hospital were registered and recorded in this study. Patients with stenosis related to radiation therapy or with restenoses after carotid endarterectomy (CEA) were excluded from the present study. All patients underwent both volumetric and cross-sectional analyses of the carotid plaque using VH IVUS. The patients who had stenosis that was too severe for the VH IVUS catheter to cross before predilatation for carotid artery stenting were also excluded from the study. The study was conducted according to the requirements of the institutional review board. The procedures of VH acquisition and periprocedural management were in agreement with the institutional guidelines.

Virtual Histology Acquisition

All procedures were performed under local anesthesia. Stenotic lesions with unstable and complex plaque were treated with proximal protection systems to avoid the risk of distal embolization by advancing the protection device and the VH IVUS

catheter through the stenosis.[28] The other lesions were treated using a distal embolic protection device. A VH IVUS was obtained before predilatation for the carotid artery stenting procedure. A VH IVUS catheter (Eagle Eye Gold, 3.5 F/20 MHz; Volcano Corporation) was placed distal to the stenotic lesion and manually pulled back proximal to the stenosis. During this pullback, color flow IVUS was recorded on the VH IVUS console. Then, the VH IVUS catheter was again advanced distal to the stenosis, and it was subsequently pulled back proximal to the stenosis by a motorized pullback system set at .5 mm/second. During this pullback, raw radiofrequency data were captured on the VH IVUS console at the top of the R-wave of the electrocardiogram and recorded on a digital video disk. Each distance between the captured images was also recorded.

Analysis of Virtual Histology

The color-coded map superimposed on the gray-scale IVUS tomographic image was reconstructed from the captured raw radiofrequency data using the VH IVUS software (version 1.3; Volcano Corporation). Using the VH IVUS software, atherosclerotic plaques were classified into the four different histological components of plaque (green, fibrous; yellow, fibrofatty; white, dense calcium; and red, necrotic core) by classification trees based on mathematical autoregressive spectral analysis of IVUS backscattered data; a VH IVUS sample image is shown in Figure 1. The distal/proximal end frames were defined as the frames where the plaque within the media line was concentric and the diameter of the lumen within the intima did not change compared with more distal/proximal frames. Between the distal and proximal end frames, a media line and an intima line were manually drawn in each frame by referring to the adjacent frames and by referring to the corresponding color flow IVUS image, respectively. Referring to adjacent frames is useful in detecting the media line. The intima line can be detected easily using the color flow IVUS images showing the blood flow in the vessel. Since the VH IVUS software could not analyze the plaque within ulceration, the ulcerated area was considered to be with an intima line in VH IVUS analyses.

The total volume of each plaque type (fibrous, fibrofatty, dense calcium, and necrotic core) was calculated using the VH IVUS software and expressed in cubic millimeters. The volumetric proportion of each plaque type was also determined. The proportion of the area of each plaque type at the minimum lumen site was also calculated using the VH IVUS software.

Statistical Analysis

A simple regression analysis was performed to examine the effects of the proportion of the four plaque types at the minimum lumen site on the volumetric proportion of each plaque type. A P value $< .05$ was considered significant. All statistical analyses were performed with the IBM SPSS statistical software package (version 19.0; SPSS Inc., Chicago, IL).

Results

Fifty-six consecutive interventional therapies for cervical carotid artery stenosis in 52 patients were initially included in this study. One patient with stenosis that was related to ra-

Table 1. Patient Data and Characteristics

Variables	Data
Clinical characteristics	
Age (years)	68.8 (SD 7.1)
Female	6 (13%)
History	
Hypertension	33 (69%)
Diabetes mellitus	20 (42%)
Hyperlipidemia	28 (58%)
Coronary artery disease	15 (31%)
Congestive heart failure	4 (8%)
Lesion-related characteristics	
Lesion side: left	25 (52%)
Distance between carotid bifurcation and MLS ≤ 10 mm	36 (75%)
Distance between carotid bifurcation and MLS > 10 mm	12 (25%)
Plaque ulceration deeper than 2 mm	19 (40%)
Stenotic lesion involving both CCA & ICA	19 (40%)
Stenotic lesion involving only ICA	29 (60%)
Degree of stenosis (%)	73.6 (SD 15.3)
Contralateral ICA stenosis (>50%) or occlusion	8 (17%)
Contralateral ICA occlusion	4 (8%)
Symptomatic carotid stenosis, ipsilateral	25 (52%)
Cerebral infarction, ipsilateral	18 (38%)
Cerebral infarction, contralateral	7 (15%)
Symptoms of carotid stenosis within 3 months, ipsilateral	11 (23%)
Cerebral infarction within 3 months, ipsilateral	7 (15%)
History of CAS or CEA, contralateral	5 (10%)

Continuous data are shown as the means (SD). Categorical data are shown as counts (%).
SD = standard deviation; MLS = minimum lumen site; CCA = common carotid artery; ICA = internal carotid artery; CAS= carotid artery stenting; CEA = carotid endarterectomy.

diation therapy and 1 patient with restenosis after CEA were excluded from the study. Since the VH analyses of the plaque were not available, six stenotic lesions (three stenoses that were too severe for the VH IVUS catheter to cross before predilatation; three stenoses in which the raw radiofrequency data captured in the VH IVUS console could not be recorded on a digital video disk because of technical difficulties) were also excluded. The remaining 48 stenotic lesions in 45 patients were analyzed in this study. The descriptive characteristics are shown in Table 1.

All patients had successful dilatation of the carotid lesion by carotid artery stenting. In the periprocedural period, no patients suffered from major adverse events, including symptomatic cerebral infarction, myocardial infarction, or death. No patients needed repeated procedures or blood transfusions after the procedure.

The volumetric proportion of each plaque type (fibrous, fibrofatty, dense calcium, and necrotic core), and the proportion of the area of each plaque type at the minimum lumen site are given in Table 2.

The scattergraphs of the volumetric proportion of each plaque type against the proportion of the corresponding plaque-type area at the minimum lumen site were drawn (Fig 2). Each

Table 2. Virtual Histology Findings

Variables	Data
Virtual Histology findings of plaque volumetric composition analysis	
Fibrous tissue (%)	61.0 (SD 12.8)
Fibrofatty tissue (%)	28.0 (SD 15.2)
Dense calcium (%)	3.9 (SD 6.2)
Necrotic core (%)	7.2 (SD 8.3)
Virtual Histology findings of plaque composition at MLS	
Fibrous tissue (%)	57.9 (SD 14.7)
Fibrofatty tissue (%)	31.6 (SD 16.8)
Dense calcium (%)	3.3 (SD 7.0)
Necrotic core (%)	7.1 (SD 9.5)

Data are shown as the means (SD).
SD = standard deviation; MLS = minimum lumen site.

regression line, the adjusted coefficient of determination, and its P value were also drawn in the graphs. The adjusted coefficients of determination of the simple regression analyses were .782 for fibrous tissue, .741 for fibrofatty tissue, .864 for dense calcium, and .918 for necrotic core, which indicated a strong correlation.

Discussion

In this study, the authors analyzed the relationship between the volumetric composition of the entire carotid plaque and the plaque composition at the minimum lumen site using simple regression analyses. The volumetric proportion of each plaque type correlated significantly with the corresponding plaque-type area at the minimum lumen site (Fig 2). This result gives support to the hypothesis that the plaque composition at the minimum lumen site represents the volumetric composition of the entire plaque that causes the stenosis.

As described earlier, periprocedural hypotension in carotid artery stenting can be predicted by VH IVUS volumetric analysis of the plaque responsible for carotid artery stenosis.[27] While VH IVUS volumetric analysis of the plaque is a time-consuming task,[3,16] analyzing only one cross-section at the minimum lumen site is easier and faster. The result of this study enables easier and faster prediction of periprocedural hypotension during carotid artery stenting, which means quick and easy analysis of the relationships between carotid plaque composition and the clinical prognosis after carotid artery stenting.

Plaque characteristics are related to not only periprocedural hypotension, but also ischemic complications in the periprocedural period of carotid artery stenting.[29] Particularly in carotid artery stenting using filter-type embolic protection devices, slow flow behavior is associated with an excess risk of periprocedural stroke and is known to be a serious complication.[25,30] Significant embolization of vulnerable plaque elements produced by the carotid artery stenting procedure is the cause of the slow flow behavior. Detecting such vulnerable plaque is important for optimizing patient and lesion selection criteria for carotid artery stenting.[31,32] CEA is one of the safer treatment options for the carotid stenosis with such vulnerable plaque. The results of this study may be useful for deciding the type of carotid
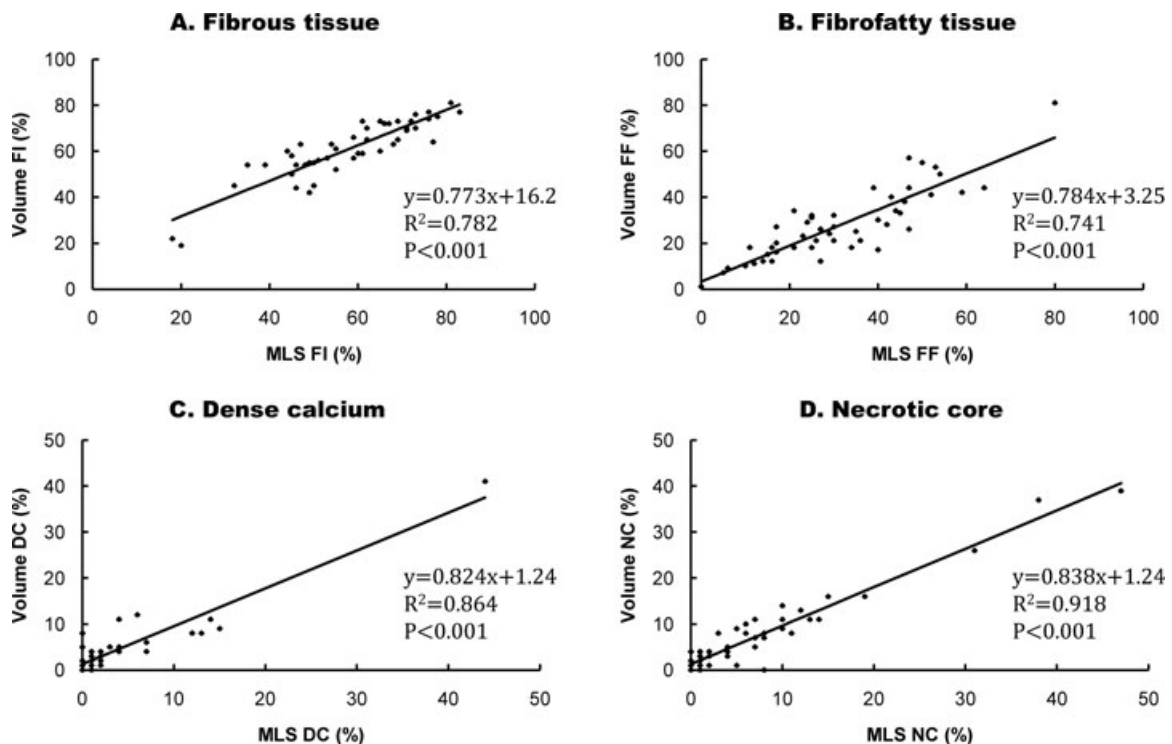
Fig 2. The scattergraphs and regression lines between the volumetric proportion of each plaque type (A) fibrous, (B) fibrofatty, (C) dense calcium, and (D) necrotic core, and the proportion of corresponding plaque-type area at the minimum lumen site. FI = fibrous; FF = fibrofatty; DC = dense calcium; NC = necrotic core; MLS = minimum lumen site; R^2 = adjusted coefficient of determination.

intervention (carotid artery stenting or CEA) using the concept of plaque-guided patient selection in carotid artery disease.[33-36]

Limitations of the Present Study

In this study, the authors analyzed only atherosclerotic plaque in cervical carotid artery stenosis. Patients with stenosis related to radiation therapy or with restenoses after CEA were excluded from this study, and there were no patients with carotid artery stenosis caused by arterial dissections in the study period. Further investigation is required for the analysis of these nonatherosclerotic plaques. In addition, VH IVUS does not identify hemorrhage within the plaque but assigns hemorrhage to fibrous or fibrofatty components via the available colors.[37,38] Hemorrhage may therefore be contained within the fibrous or fibrofatty components assessed by VH IVUS.[25] The risk of intraplaque hemorrhage should be assessed by combination use of other plaque-imaging devices.

Conclusions

The result of this study indicates that the plaque composition at the minimum lumen site represents the volumetric composition of the entire carotid plaque responsible for atherosclerotic cervical carotid artery stenosis; this may be useful for deciding the type of carotid intervention using the concept of plaque-guided patient selection in carotid artery disease.

References

1. Biasi GM, Froio A, Diethrich EB, et al. Carotid plaque echolucency increases the risk of stroke in carotid stenting: the Imaging in Carotid Angioplasty and Risk of Stroke (ICAROS) study. *Circulation* 2004;110:756-762.
2. Gronholdt ML, Nordestgaard BG, Schroeder TV, et al. Ultrasonic echolucent carotid plaques predict future strokes. *Circulation* 2001;104:68-73.
3. Diethrich EB, Pauliina Margolis M, Reid DB, et al. Virtual histology intravascular ultrasound assessment of carotid artery disease: the Carotid Artery Plaque Virtual Histology Evaluation (CAPITAL) Study. *J Endovasc Ther* 2007;14:676-686.
4. Esposito L, Saam T, Heider P, et al. MRI plaque imaging reveals high-risk carotid plaques especially in diabetic patients irrespective of the degree of stenosis. *BMC Med Imaging* 2010;10:27.
5. Kurosaki Y, Yoshida K, Endo H, et al. Association between carotid atherosclerosis plaque with high signal intensity on T1-weighted imaging and subsequent ipsilateral ischemic events. *Neurosurgery* 2011;68:62-67.
6. Yamada K, Yoshimura S, Kawasaki M, et al. Embolic complications after carotid artery stenting or carotid endarterectomy are associated with tissue characteristics of carotid plaques evaluated by magnetic resonance imaging. *Atherosclerosis* 2011;215:399-404.
7. Young VE, Patterson AJ, Sadat U, et al. Diffusion-weighted magnetic resonance imaging for the detection of lipid-rich necrotic core in carotid atheroma in vivo. *Neuroradiology* 2010;52:929-936.
8. Homburg PJ, Rozie S, van Gils MJ, et al. Association between carotid artery plaque ulceration and plaque composition evaluated with multidetector CT angiography. *Stroke* 2011;42:367-372.
9. He C, Yang ZG, Chu ZG, et al. Carotid and cerebrovascular disease in symptomatic patients with type 2 diabetes: assessment of prevalence and plaque morphology by dual-source computed tomography angiography. *Cardiovasc Diabetol* 2010;9:91.
10. Derlin T, Wisotzki C, Richter U, et al. In vivo imaging of mineral deposition in carotid plaque using 18F-sodium fluoride PET/CT: correlation with atherogenic risk factors. *J Nucl Med* 2011;52:362-368.
11. Moustafa RR, Izquierdo Garcia D, Fryer TD, et al. Carotid plaque inflammation is associated with cerebral microembolism in patients with recent transient ischemic attack or stroke: a pilot study. *Circ Cardiovasc Imaging* 2010;3:536-541.
12. Meyers PM, Schumacher HC, Gray WA, et al. Intravascular ultrasound of symptomatic intracranial stenosis demonstrates atherosclerotic plaque with intraplaque hemorrhage: a case report. *J Neuroimaging* 2009;19:266-270.
13. Ravalli S, LiMandri G, Di Tullio MR, et al. Intravascular ultrasound imaging of human cerebral arteries. *J Neuroimaging* 1996;6:71-75.
14. Nair A, Kuban BD, Tuzcu EM, et al. Coronary plaque classification with intravascular ultrasound radiofrequency data analysis. *Circulation* 2002;106:2200-2206.
15. Nair A, Calvetti D, Vince DG. Regularized autoregressive analysis of intravascular ultrasound backscatter: improvement in spatial accuracy of tissue maps. *IEEE Trans Ultrason Ferroelectr Freq Control* 2004;51:420-431.
16. Nasu K, Tsuchikane E, Katoh O, et al. Accuracy of in vivo coronary plaque morphology assessment: a validation study of in vivo virtual histology compared with in vitro histopathology. *J Am Coll Cardiol* 2006;47:2405-2412.
17. Rodriguez-Granillo GA, Vaina S, Garcia-Garcia HM, et al. Reproducibility of intravascular ultrasound radiofrequency data analysis: implications for the design of longitudinal studies. *Int J Cardiovasc Imaging* 2006;22:621-631.
18. Vince DG, Davies SC. Peripheral application of intravascular ultrasound virtual histology. *Semin Vasc Surg* 2004;17:119-125.
19. Rodriguez-Granillo GA, Bruining N, Mc Fadden E, et al. Geometrical validation of intravascular ultrasound radiofrequency data analysis (Virtual Histology) acquired with a 30 MHz boston scientific corporation imaging catheter. *Catheter Cardiovasc Interv* 2005;66:514-518.
20. Rodriguez-Granillo GA, Serruys PW, Garcia-Garcia HM, et al. Coronary artery remodelling is related to plaque composition. *Heart* 2006;92:388-391.
21. Wehman JC, Holmes DR Jr, Ecker RD, et al. Intravascular ultrasound identification of intraluminal embolic plaque material during carotid angioplasty with stenting. *Catheter Cardiovasc Interv* 2006;68:853-857.
22. Takayama K, Taoka T, Nakagawa H, et al. Successful percutaneous transluminal angioplasty and stenting for symptomatic intracranial vertebral artery stenosis using intravascular ultrasound virtual histology. *Radiat Med* 2007;25:243-246.
23. Tsurumi A, Tsurumi Y, Negoro M, et al. Subcutaneous hematoma associated with manual cervical massage during carotid artery stenting. A case report. *Interv Neuroradiol* 2011;17:386-390.
24. Irshad K, Millar S, Velu R, Reid AW, et al. Virtual histology intravascular ultrasound in carotid interventions. *J Endovasc Ther* 2007;14:198-207.
25. Matsumoto S, Nakahara I, Higashi T, et al. Fibro-fatty volume of culprit lesions in Virtual Histology intravascular ultrasound is associated with the amount of debris during carotid artery stenting. *Cerebrovasc Dis* 2010;29:468-475.
26. Rodriguez Granillo GA, Garcia Garcia HM, Mc Fadden EP, et al. In vivo intravascular ultrasound-derived thin-cap fibroatheroma

detection using ultrasound radiofrequency data analysis. *J Am Coll Cardiol* 2005;46:2038-2042.

27. Tsurumi A, Miyachi S, Hososhima O, et al. Can periprocedural hypotension in carotid artery stenting be predicted? A carotid morphologic autonomic pathologic scoring model using virtual histology to anticipate hypotension. *Interv Neuroradiol* 2009;15:17-28.

28. Parodi JC, Ferreira LM, Sicard G, et al. Cerebral protection during carotid stenting using flow reversal. *J Vasc Surg* 2005;41:416-422.

29. Tubler T, Schluter M, Dirsch O, et al. Balloon-protected carotid artery stenting: relationship of periprocedural neurological complications with the size of particulate debris. *Circulation* 2001;104:2791-2796.

30. Casserly IP, Abou Chebl A, Fathi RB, et al. Slow-flow phenomenon during carotid artery intervention with embolic protection devices: predictors and clinical outcome. *J Am Coll Cardiol* 2005;46:1466-1472.

31. Inglese L, Fantoni C, Sardana V. Can IVUS-virtual histology improve outcomes of percutaneous carotid treatment? *J Cardiovasc Surg (Torino)* 2009;50:735-744.

32. Schiro BJ, Wholey MH. The expanding indications for virtual histology intravascular ultrasound for plaque analysis prior to carotid stenting. *J Cardiovasc Surg (Torino)* 2008;49:729-736.

33. Yoshimura S, Yamada K, Kawasaki M, et al. High-intensity signal on time-of-flight magnetic resonance angiography indicates carotid plaques at high risk for cerebral embolism during stenting. *Stroke* 2011;42:3132-3137.

34. van Lammeren GW, Reichmann BL, Moll FL, et al. Atherosclerotic plaque vulnerability as an explanation for the increased risk of stroke in elderly undergoing carotid artery stenting. *Stroke* 2011;42:2550-2555.

35. Yoshimura S, Kawasaki M, Hattori A, et al. Demonstration of intraluminal thrombus in the carotid artery by optical coherence tomography: technical case report. *Neurosurgery* 2010;67:onsE305.

36. Hao H, Iihara K, Ishibashi Ueda H, Saito F, et al. Correlation of thin fibrous cap possessing adipophilin-positive macrophages and intraplaque hemorrhage with high clinical risk for carotid endarterectomy. *J Neurosurg* 2011;114:1080-1087.

37. Nasu K, Tsuchikane E, Katoh O, et al. Impact of intramural thrombus in coronary arteries on the accuracy of tissue characterization by in vivo intravascular ultrasound radiofrequency data analysis. *Am J Cardiol* 2008;101:1079-1083.

38. Hishikawa T, Iihara K, Ishibashi Ueda H, et al. Virtual histology-intravascular ultrasound in assessment of carotid plaques: ex vivo study. *Neurosurgery* 2009;65:146-152.